Current Journal of Applied Science and Technology

Volume 43, Issue 1, Page 46-58, 2024; Article no.CJAST.112025
ISSN: 2457-1024
(Past name: British Journal of Applied Science & Technology, Past ISSN: 2231-0843, NLM ID: 101664541)

Monitoring the Air-fuel Ratio (AFR) of a Biomass Gasification Process with an Arduino Uno 3 and a Narrow Band Lambda Oxygen Sensor

Hamidou Salou [a*], Nzihou Jean Fidele [b], Zoundi Ousmane [b], Ouattara Frederic [b] and Segda Bila Gerard [c]

[a] Catholic University of West Africa, University Unit in Bobo-Dioulasso, Bobo-Dioulasso, Burkina Faso.
[b] Analytical Chemistry, Spatial Physics and Energetic Laboratory, Norbert Zongo University, Koudougou, Burkina Faso.
[c] Environnemental Physic and Chemistry Laboratory, Joseph Ki-Zerbo University, Ouagadougou, Burkina Faso.

Authors' contributions

This work was carried out in collaboration among all authors. All authors read and approved the final manuscript.

Article Information

DOI: 10.9734/CJAST/2024/v43i14344

Open Peer Review History:
This journal follows the Advanced Open Peer Review policy. Identity of the Reviewers, Editor(s) and additional Reviewers, peer review comments, different versions of the manuscript, comments of the editors, etc are available here: https://www.sdiarticle5.com/review-history/112025

Original Research Article

Received: 16/11/2023
Accepted: 22/01/2024
Published: 25/01/2024

ABSTRACT

The Air-Fuel Ratio is one of the keys parameters for driving the gasification process. Monitoring of oxygen percentage in flue gases is one of various ways of controlling efficiency and emissions of industrial combustion. Biomass gasification is a thermochemical degradation of the biomass that is accomplished with the Air-Fuel Ratio less than the stochiometric one that is used in the combustion.
Unfortunately, flue gases analyzers in combustion processes are expensive and not accessible to small scale industries. This is particularly true in developing countries. The Lambda sensor used in

**Corresponding author: E-mail: h_salou@yahoo.fr;*

the automotive industry is an oxygen sensor which controls the electronic injection of the modern internal combustion vehicles.
The aim of this study is to present one simple method of measuring the oxygen concentration and calculate the Air-Fuel Ratio in synthesis gas produced by a downdraft biomass gasifier by the use of an Arduino Uno 3 microcontroller and an automotive Lambda sensor. This method use the voltage signals developed by a heated 4 wires Lambda sensor and the Nernst Equation to calculate oxygen concentration in the producer gas and derive the Air-Fuel Ratio.
Results presented in this article show that this method is a simple and cost-effective way to monitor Air-Fuel Ratio in a biomass gasifier.

Keywords: Air-fuel ratio; biommas; gasification; lambda sensor; Arduino.

1. INTRODUCTION

Biomass gasification is used very little in Burkina Faso, although it has proven to be one of the most efficient methods for converting biomass into thermal and electrical energy. Despite the abundance of waste of agricultural, plant and household origin, the large-scale recovery of this conversion process is very little developed in Burkina Faso. [1,2]. In a bibliographic review made in 2014, it was established that gasification of waste may be an interesting alternative for waste valorization in Burkina Faso [3] Other studies on the development of biomass energy in Africa agree with the main conclusions of that review [4-6].

The equivalence ratio (ER) of a system is defined as the ratio of the hydrocarbon-to-oxidizer ratio to the stoichiometric hydrocarbon-to-oxidizer ratio which can be expressed with equation (1) below :

$$\boldsymbol{ER} = \frac{(fuel\ to\ oxidize\ ratio)_{act}}{(fuel\ to\ oxidizer\ ratio)_{sto}} = \frac{[m_{fuel}/(m_{oxy})]_{act}}{[m_{fuel}/(m_{oxy})]_{sto}} = \frac{[n_{fuel}/(n_{oxy})]_{act}}{[n_{fuel}/(n_{oxy})]_{sto}} \quad (1)$$

In equation (1), m represents the mass, n represents number of moles. Subscripts *act* and *sto* refer to actual and stoichiometric ratios respectively for the corresponding mass or mole fractions.

According to Vaclav et al. [7] : if air is used as the oxidizer, equation (1) can be rewritten as follow :

$$\boldsymbol{ER} = \frac{(fuel\ to\ oxidizer\ ratio)_{act}}{(fuel\ to\ oxidizer\ ratio)_{sto}} = \frac{[m_{fuel}/(m_{air})]_{act}}{[m_{fuel}/(m_{air})]_{sto}} = \frac{[n_{fuel}/(n_{air})]_{act}}{[n_{fuel}/(n_{air})]_{sto}} \quad (2)$$

Air Fuel Ratio is given by equation 3 below :

$$\boldsymbol{AFR} = \frac{m_{air}}{m_{fuel}} = \frac{\rho_{air}.V_{air}}{\rho_{fuel}.V_{fuel}} = \frac{1}{d}\frac{V_{air}}{V_{fuel}} \quad (3)$$

Where ρ is the, V is the volume, d is the density of the fuel against air.

Comparing equations 3 and 2, we see that ER is the ratio of the stoichiometric AFR to the actual AFR.

Commercial Lambda sensors give the excess oxygen in the flue gas. Therefore, we can compute the AFR from the output of the Lambda sensor.

In an experimental study on air gasification of polypropylene, Xiao et al.[8] studied the effect of the ER and found that equivalence ratio appeared to have a significant effect on the reactor temperature and other gasification results. The increase of the equivalence ratio favored the formation of the fuel gas and decreased the formation of the tars and char. Other authors obtained similar results [9-11]. Coming out as a summary, the work done by Vaezi et al. [12] used the thermochemical equilibrium modeling to predict the performance of a heavy fuel oil gasifier. Their model combined both the chemical and thermodynamic equilibriums of the global gasification reaction in order to predict the final syngas species distribution. They compared the results of their simulations with reported experimental measurements through which their numerical model was validated. They found that the ER exhibit an optimum value respective to producer gaz yield as depicted on Fig 1.

Therefore, monitoring of the ER, i.e the AFR appear of the up most importance in the gasification process. We have designed and tested two wood fired downdraft biomass gasifier in Burkina Faso [13],[14]. Unfortunately, we were limited by the failure of the five flue gas analyzers we have on hands and even the replacement of the oxygen or carbon monoxide sensors appeared out of reach, because these are relatively costly and not suited for long run usage (maximum 5 minutes recommended by the

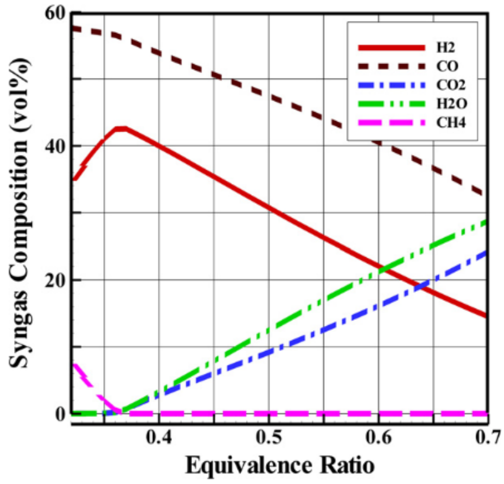

Fig. 1. Effect of the ER on the producer gas composition (from Vaezi et al. [12]

manufacturers). Therefore, we looked around and found that several authors used Lambda sensors to monitor the excess air and other gases in industrial applications [15-18]. We also found that the Arduino microcontroller can be used to acquire data from numerous sensors, compute several mathematical functions and display or log these values in an USB drive [19-23].

Using Lambda sensors and the Arduino microcontroller emerged as very interesting and cost effective replacement solution for monitoring the ER in our biomass gasifiers.

2. MATERIALS AND METHODS

2.1 Experimental Setup

Overview of the experimental setup is given on Fig 2.

Technical specifications of the Arduino Uno 3 development board are given in Table 1.

2.2 Methods

2.2.1 Determination of the temperature

A K type thermocouple is used along with its amplification and analog to digital converter referenced as Max6675 to acquire the working temperature of the gasifier in °C where the Lambda sensor is plugged in. Conversion in K is made in the Arduino Integrated Development Environment (IDE).

2.2.2 Determination of the oxygen concentration

A zirconium oxide oxygen sensor, as for example the commercial narrowband Lambda sensor found in automotives, consists of a pair of porous platinum electrodes separated by a layer of the zirconium oxide as illustrated by Najjar et al. [24] on Fig 3.a.

At high temperatures (above 573K) the zirconium ceramic becomes conductive to oxygen ions. The Lambda sensor is made in the way that the sensing side is plugged into the monitored device, while exposition to air is internally assured through the unplugged part of the sensor (Fig 3.b). When exposed to two different levels of oxygen concentration on either side of the cell, for example : one side to gas exhaust and another to the ambient air, an electro-motive force (emf) voltage is produced. Partial pressures of oxygen in addition to temperature and the emf can therefore be used to determine air/fuel ratio for an exhaust stream from a combustion system when referenced to the known ambient oxygen concentration in air.

The analog signal output from the Lambda sensor computed by Lutero C. de Lima et al. [25] varies from 0 to 80mV around 800°C. At 500°C they found 28mV at 4% and 7.5mV at 15%. Our Arduino board use a 12 bits analog to digital conversion from 0 to 5V. Taking in account that gasification is conducted under sub-stoichiometric conditions, we limit our self to oxygen content from 3% to 15% at 850°C. Therefore, we need a maximal analog signal amplification gain of 5000mV/80mV = 62.5.

Table 1. Arduino Uno 3 technical specifications

Microcontroller	ATmega328P
Operating Voltage	5V
Input Voltage (recommended)	7-12V
Input Voltage (limit)	6-20V
Digital I/O Pins	14 (of which 6 provide PWM output)
PWM Digital I/O Pins	6
Analog Input Pins	6
DC Current per I/O Pin	20 mA
DC Current for 3.3V Pin	50 mA
Flash Memory	32 KB (ATmega328P) of which 0.5 KB used by bootloader
SRAM	2 KB (ATmega328P)
EEPROM	1 KB (ATmega328P)
Clock Speed	16 MHz
LED_BUILTIN	13
Length	68.6 mm
Width	53.4 mm
Weight	25 g

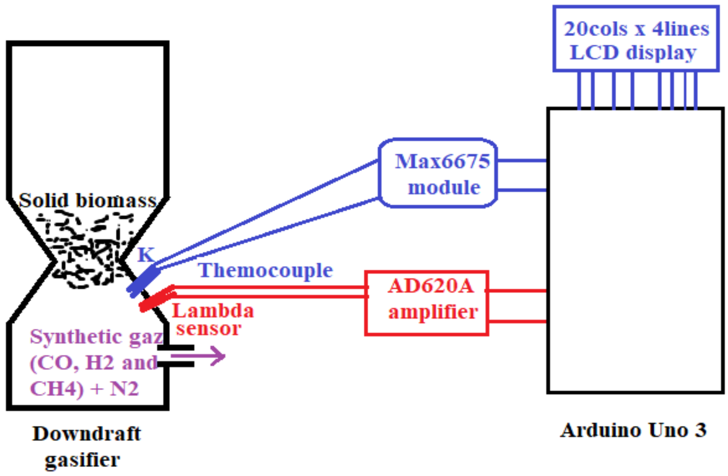

Fig. 2. Experimental setup

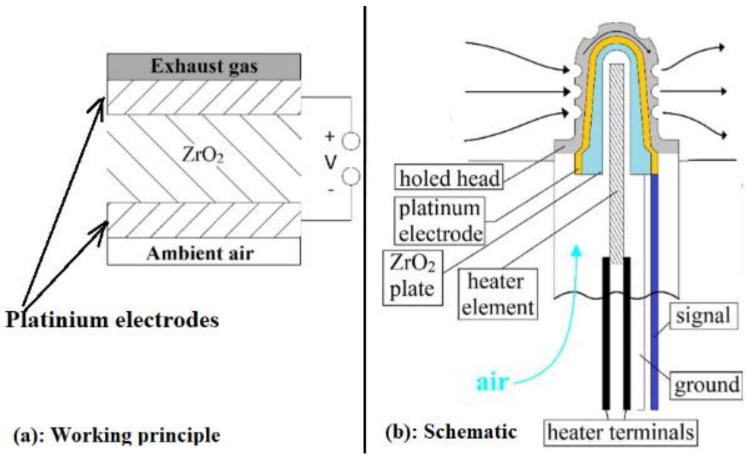

Fig. 3. Working principle and schematic diagram of a Lambda oxygen sensor, from Najjar et al. [24]

Figures Fig 4 depict the AD620 low power µV and mV signal amplifier we used to amplify the emf supplied by the Lambda sensor.

Amplified analog signal from the Lambda sensor was directed to an analog input pin of the Arduino Uno 3 board as illustrated on Fig 5.

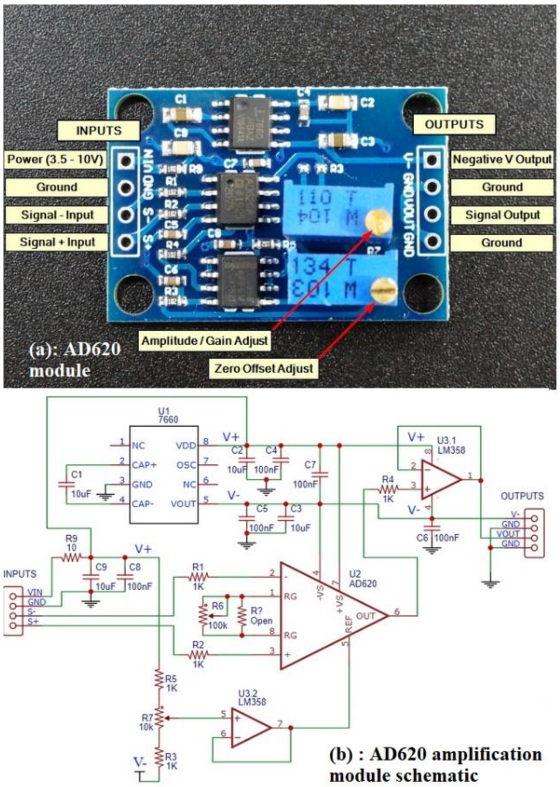

Fig 4. The AD620 module and schematic

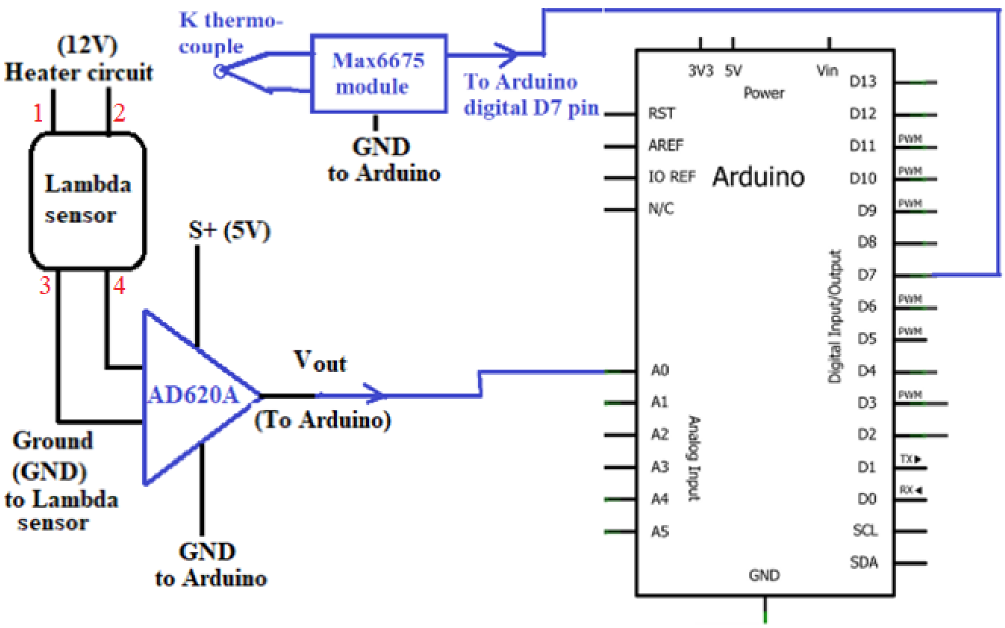

Fig. 5. Electrical diagram of the monitoring system

Pins 1 and 2 of the Lamda sensor on Fig 5 are of black color and are those of the heater element. These pins are connected to 12V DC. When heater element is powered, the DC current read in the order of 0.9A, which give a cold heater resistance of 12V/0.9 = 13.33Ω. This heater element resistance increases over time. Heat released by this heater element make the porous ZrO2 element to become conductive at temperatures above 360°C. But for accurate readings, the manufacturers recommend and operating temperature of 600°C.

Pins 3 and 4 on Fig 5 are the signal pins. Pin 3 of with color is the negative of the emf produced by the Lambda sensor whereas pin 4 is of white color and is the positive of that produced emf. Oxygen concentration is determined through the Nernst Law:

$$O_2(\%) = 20.96 \exp\left(-\frac{zF}{RT}\,E\right) \quad (4)$$

20.96 is the volumic concentration of oxygen in clean air,

z is the number of electrons migrating between the sensor electrodes,
F is the Faraday constant,
E is the amplified voltage developed across the sensor terminals,
R is the universal constant of ideal gases,
T is the absolute temperature in the Lambda sensor.

A commercial heated 4 wires Lambda sensor was installed in the reduction zone of a downdraft gasifier. Close to the Lambda sensor was installed a type K thermocouple. A simple, electrical circuit comprising a 5V DC power source in serie with an amperemeter and the heating element of the Lambda sensor was used. An electronic voltmeter was attached in parallel to the heating element. An oscilloscope was also attached to the signal wires of the Lambda sensor as shown in Fig 5.

Basically, the heating element is driven with an electronic circuit to supervises the electrical resistance of the sensor's heater. That electronic control was not used in this paper and will be implemented through the use of the Pulse Wide Modulation (PWM) technic in another upcoming paper.

The heater element resistance variation across the time is represented on Fig 7.

2.2.3 Determination of the AFR

AFR is calculated using equation (3). We must first find the stoichiometric AFR of wood in clean air. Wood composition slightly varies between species, but can be in first approximation represented as $C_6H_{12}O_5$, when wood is supposed not to contain nitrogen or minerals.

The stoichiometric combustion of wood in air containing 21% of oxygen and 79% of nitrogen is the following:

$$C_6H_{12}O_5 + 6.5(O_2 + 4.77N_2) \xrightarrow{yields} 6H_2O + 6CO_2 + 31N_2 \quad (4)$$

Stoichiometric AFR correspond to 21% of oxygen. Actual AFR, $(AFR)_{act}$ correspond to percent of oxygen given by the lambda sensor according to equation (3). We the derive equation below:

$$(AFR)_{act} = \frac{oxygen(\%)}{20.96}(AFR)_{sto} \quad (5)$$

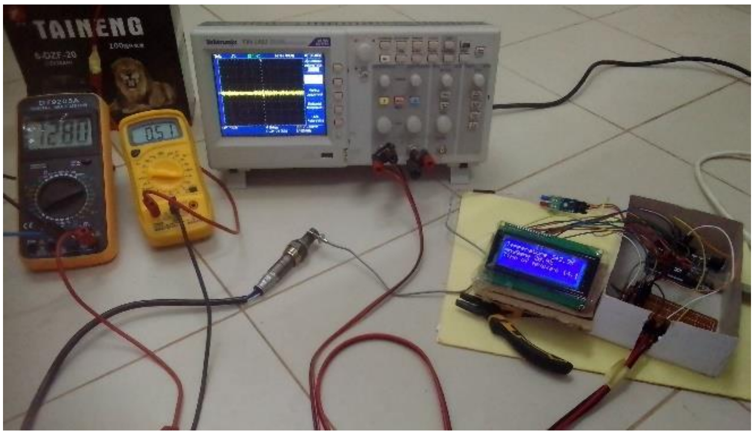

Fig. 6. Heater circuit resistance determination setup

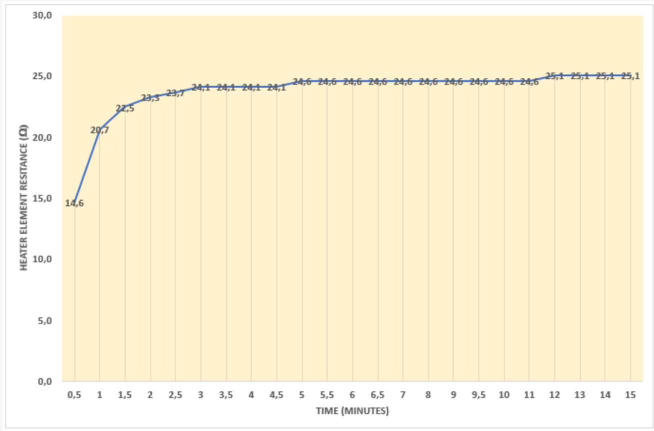

Fig. 7. Variation of the resistance of the heating element inside the Lambda sensor during the application of an 5V DC power supply

3. RESULTS AND DISCUSSION

3.1 Calibration of the Lambda Sensor

The Lambda sensor doesn't require a complicated or costly calibration but the heater resistance of a Lambda sensor widely vary from a supplier to another. We thus first checked the response of the heating element during the application of a continuous electrical power aiming to set the required working temperature of the Lambda sensor to more than 600 ºC and to check the Lambda sensor is working as intended. Fig 5 show the setup for that setup.

The response of the Lambda sensor to a DC power supply is shown on Fig 7

We can see in Fig 7 that the resistance of our Lambda sensor vary from 14.5Ω to 25.1Ω and is stabilized after 5 minutes of heating.

This is because the final temperature of the heater element depends on the power energy it receives and heat radiation in the flue gaz. This is because the sensing element is a porous substrate and heat flow from high to lower temperatures. If it happens that flue gas his hotter than the heater element, the last will receive heat from the flue gas. Therefore, temperature of the flue gas also impacts the heater resistance. This is why, the heater element should be managed with an appropriate electronic circuit that aim to maintain the heating element at the correct working temperature.

Gibson et al. [26] and Varamban et al. [27] , using the Current Reversal Mode aimed at improving the accuracy of the measured oxygen content combustion system reported that until 12% of oxygen the correlation is perfect and from 15% up another correlation showed itself perfect, characterizing a transitional behavior of the Lambda sensor at the range from 12 to 15%.

Using the same method and comparing against measurements taken from the reference combustion analyzer (Testo 300 XL) Lutero C. de Lima et al. [25], found that the average deviation of the set of measurements was of ±5% and the correlation factor was of 0.97 demonstrating good agreement between the measurement of oxygen concentration at the flue gases and the measurements made by the reference monitor.

In the case of gasification process, we work in sub-stoichiometric conditions. Therefore, we are under 14.7% of stoichiometric combustion of gasoline.

Table 2. The heater element resistance varies with the temperature over the time as we can see on

Time (s)	0,5	2	4	6	8	10	12	14	16
R (Ω)	14,6	23,3	24,1	24,6	24,6	24,6	25,1	25,1	25,1
Tempe-rature(°C)	33	35,6	45	55	62	66	69	70	70,1

First generation of Lambda sensors are 4 wires sensors, whereas the second generation have 5 wires and are called wideband, because these can measure a wider range of oxygen concentration in flue gaz. Narrowband sensors output an emf of 100mV to 900mV. They don't need extra electronic circuitry other than for the heating element. Wideband Lambda sensors output an emf of 0 to 5V. These sensors must use proprietary modules to work. Better to avoid them in the context of monitoring biomass gasification, because narrowband sensors does the job. We conclude that a narrowband Lambda sensor for measuring oxygen content when monitoring biomass gasification is largely sufficient and accuracy have been supposed based on results in references [15], [25], [26] and [27].

3.2 Computing and Displaying AFR

Detailed code is given in appendix. Results obtained are displayed on a 20 columns with 4 lines LCD display as seen in Fig 8.

In equation 4 above, mass of wood is m_{wood} =164g.

Required mass of air for stoichiometric combustion is m_{air} = 642.07g.

Hence the stoichiometric AFR is :

$(AFR)_{sto}$ = 642.07/164 = 3.91, and also
$(AFR)_{act}$ = (3.91/20.97) O_2(%), which give:
AFR= 0.1865xO2(%)

Reciprocally:

O2(%) = AFR/0.1865

According to work of Sahar Safiran et al. [28], optimum AFR for wood and woody biomass gasification was comprised between 1.8 and 2. We computed oxygen excess againt AFR and obtained Fig 9.

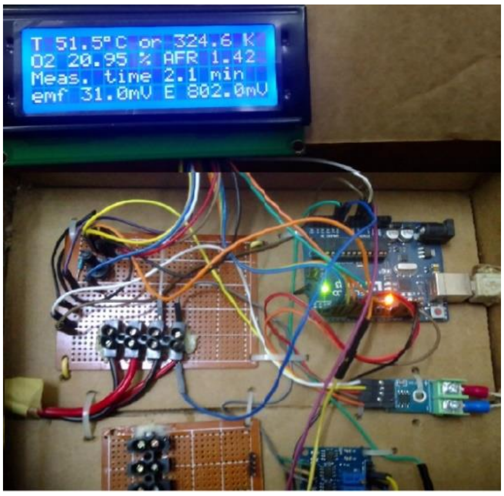

Fig. 8. Finisesh prototype with LCD display

With these results, we can see that monitoring the AFR give us an idea on how well the gasification process is running. As a perspective, we see the possibility of automatically controlling the AFR through a control loop which could give a correction signal through the PWM in order to control the primary air flow of the gasifier thus adjust the AFR.

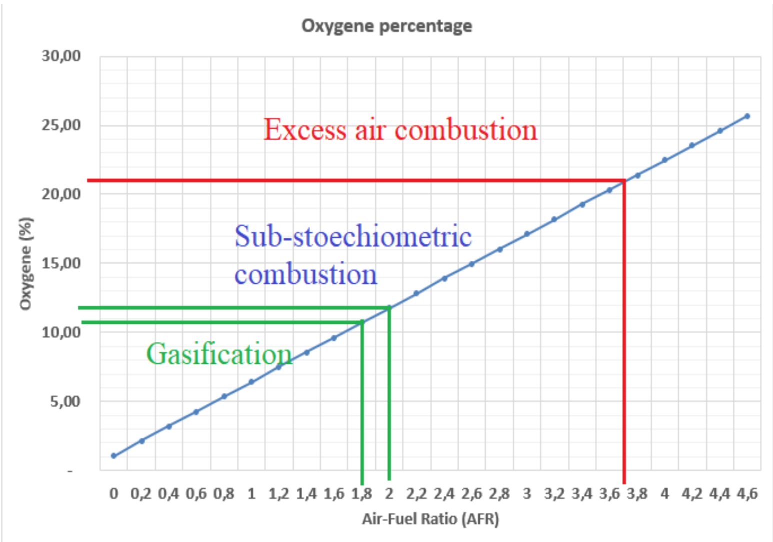

Fig. 9. Oxygene excess as function of AFR

4. CONCLUSION

A preliminary heating time of 5 minutes is required before the resistance of the heating element was stabilized. This heating time is necessary to bring the sensing element of the Lambda sensor at temperatures above 360C where the sensing element become conductive and begin to output an emf that is measured in order to calculate oxygen concentration. This work present simple methods for acquiring temperature and oxygen concentration with sensors and an Arduino board. Using the Arduino Integrated Development Environment (IDE), we successfully programmed the Arduino Uno 3 board in C++, measured both the Lambda sensor temperature with a K type thermocouple, the emf developed by the Lambda sensor and the amplified signal E. We calculated O2 concentration, derived the AFR and displayed temperature T (°C and K), O2 (%), AFR, Time of Measure (minutes), emf (mV) and E (mV) on an user friendly 20x4 LCD display. An upcoming paper will address the stabilization of the heating element resistance at a given temperature, when working temperature fluctuate through the use of Pulse Wide Modulation (PWM).

COMPETING INTERESTS

Authors have declared that no competing interests exist.

REFERENCES

1. Sustainable Energy for All, [Burkina Faso]: Rapid Assessment and Gap Analysis. 2023;1-2, Available:https://www.seforall.org/sites/default/files/Burkina_Faso_RAGA_FR_Released.pdf
Accessed on 26 septembre 2023. French.
2. Joan Nyika, Adeolu Adesoji Adediran, Adeniyi Olayanju, Olanrewaju Seun Adesina and Francis Odikpo Edoziuno, The potential of biomass in africa and the debate on its carbon neutrality, Biotechnological Applications of Biomass; 2020
DOI: 10.5772/intechopen.93615,
3. Nzihou Jean Fidele, Koulidiati Jean, Segda B. Gérard. Potential and feasibility of solid municipal waste treatment with Gasifiers in a Developing Country: A Review for Burkina Faso British Journal of Applied Science & Technology. 2014;4(3):450-464, Available:www.sciencedomain.org
4. Wood-Based Biomass Energy Development for Sub-Saharan Africa: Issues and Approaches.
Available:https://openknowledge.worldbank.org/entities/publication/9bb75b9a-7102-513b-99be-4895fbff7e2f;
Available:http://hdl.handle.net/10986/26149
5. VENRO, Rethinking Biomass Energy in Sub-Sahara Africa; 2009.
Available:https://venro.org/fileadmin/user_upload/Dateien/Daten/Publikationen/Factsheets/2009_Afrika_EU_Bioenergiestudie_englisch.pdf 2009
6. Belynda Petrie, Duncan J Macqueen, South African biomass energy: Little heeded but much needed, IIED Briefing. 2013;4.
Available:https://www.iied.org/sites/default/files/pdfs/migrate/17165IIED.pdf August 2013
7. Václav Nevrlý, Michal Dostál, Zdeněk Zelinger, Ultra-lean combustion mode in Fundamentals of Low Emission Flameless Combustion and Its Applications. 2022;13-43,
Available:https://doi.org/10.1016/c2020-0-02292-9,
8. Rui Xiao, Baosheng Jin, Air gasification of polypropylene plastic waste in fluidized bed gasifier, Energy Conversion and Management. 2007;48(3):778-786, Available:https://doi.org/10.1016/j.enconman.2006.09.004, 2007
9. Woranuch Jangsawang, Krongkaew Laohalidanond, Somrat Kerdsuwan, Optimum Equivalence Ratio of Biomass Gasification Process Based on Thermodynamic Equilibrium Model, International Conference on Alternative Energy in Developing Countries and Emerging Economies, Energy Procedia. 2015;79:520 – 527.
10. 1 S.A. Salaudeen, P. Arku, Animesh Dutta, Chapter 10 - Gasification of Plastic Solid Waste and Competitive Technologies, Fuel, Chemicals, and Sustainability Implications, Plastics Design Library. 2019;269-293,
11. Arena U, Chapter 17 : Fluidized bed gasification, Fluidized bed technologies for near-zero emission. Combustion and Gasification, Volume in Woodhead Publishing Series in Energy. 2013;765-812 Available:https://www.sciencedirect.com/science/article/pii/b9780857095411500170

12. M. Vaezi, M. Passandideh-Fard, M. Moghiman, M. Charmchi, Gasification of heavy fuel oils: A thermochemical equilibrium approach. Fuel. 2010;90:878-885.
DOI :http://dx.doi.org/10.1016/j.fuel.
13. Nzihou Jean Fidele, Hamidou Salou, Imbga Kossi, Segda Bila Gerard, Ouattara Frederic, Tiemtore Hamadou, Electrical power generation from heat recovered at the throat of a downdraft biomass Gasifier, American Journal of Science, Engineering and Technology. 2023;8(3): 133-140,
Available:http://www.sciencepublishinggroup.com/j/ajset
DOI: 10.11648/j.ajset.20230803.12, ISSN: 2578-8345 (Print); ISSN: 2578-8353
14. Nzihou Jean Fidele, Hamidou Salou, Segda Bila Gerard, Ouattara Frederic and Compaore Hamidou, Effects of a cyclone dimensions on quality of syngas produced with a wood-fired biomass gasifier, Journal of Energy Research and Reviews. 2023;15(3):1-14.
Article number JENRR.107030, ISSN: 2581-8368.
15. Antonio S. de Souza Sobrinho, Francisco S. Cavalcante Junior and Lutero C. de Lima, Monitoring Industrial Combustion Through Automotive Oxygen Sensor, International Transaction Journal of Engineering, Management, & Applied Sciences & Technologies. 2015;3(2).
ISSN 2228-9860, eISSN 1906-9642.
Available:http://TuEngr.com/V03/203-211.
16. S Aravind, P Ragupathi, D Sathish Kumar, G Vignesh, A Numerical Investigation of Automotive Lambda Sensor to Improve the Life Span of the Sensor using CFD, IOP Conferences Series: Materials Science and Engineering. IOP Publishing. 2020; 012003
DOI:10.1088/1757-899X/923/1/012003.
17. Sleight Halley, Kannan Pasupathikovil Ramaiyan, Lok-kun Tsui, Fernando Garzon, A review of zirconia oxygen, NOx, and mixed potential gas sensors – History and current trends, Sensors and Actuators B: Chemical. 2022;370(1).
Available:https://doi.org/10.1016/j.snb.2022.132363.
18. Brailsford AD, Yussouff M, Logothetis EM, Shane M, Steady-state model of a zirconia oxygen sensor in a simple gas mixture, Sensors and Actuators B: Chemical.1995;25(1-3):362-365.
19. Nasir AY, Bature UI, Tahir NM, Babawuro AY, Boniface A, Hassan AM, Arduino based gas leakage control and temperature monitoring system. International Journal of Informatics and Communication Technology (IJICT). 2020;9(3):171-178.
20. ISSN: 2252-8776,
DOI: 10.11591/ijict.v9i3.pp171-178
21. Sabr Ahmed, Intelligent Bio-Detector, Open Journal of Applied Sciences. 2016;6:903-937.
DOI: 10.4236/ojapps.2016.613078
December 28, 2016
22. Abubakar Yakub Nasir, Bature UI, Tahir NM, Babawuro AY, Adoyi Boniface AM. Hassan, Arduino based gas leakage control and temperature monitoring system, International Journal of Informatics and Communication Technology (IJ-ICT). 2020;9(3):171-178.
ISSN : 2252-8776,
DOI : 10.11591/ijict.v9i3.
Available:http://ijict.iaescore.com
23. Huan Hui Yan, Yusnita Rahayu, Design and development of gas leakage monitoring system using Arduino and ZigBee, Proceeding of International Conference on Electrical Engineering, Computer Science and Informatics (EECSI 2014), Yogyakarta, Indonesia; 2014.
24. Dewi L, Somantri Y, Wireless sensor network on lpg gas leak detection and automatic gas regulator system using Arduino, IOP Conf. Serie: Material Sciences Engeeniring. 2018;384: 012064
25. Yousef SH, Najjar, Abad Alrahman WH, Almardini Amro JA, Sawan, Comparison of performance using wide-band versus narrow-band oxygen sensors in gasoline engines, Case Studies in Thermal Engineering, Elsevier Ltd; 2019.
Available:https://doi.org/10.1016/j.csite.2019.100552
26. Lutero C. de Lima, Humberto A. Carmona, Cesar V. M. da Silva and Francisco S. Cavalcante Junior, Oxygen Excess Control of Industrial Combustion Through the Use of Automotive Lambda Sensor, International Transaction Journal of Engineering, Management, & Applied Sciences & Technologies. 2011; 2(3).
ISSN 2228-9860. eISSN 1906-9642.
Available:http://TuEngr.com/V02/365-373.
27. Gibson RW, Kumar RV, Fray DJ. Novel sensors for monitoring high oxygen

concentrations. Solid State Ionics.1999; 121:43-50,

28. Varamban, S.V., R. Ganesan and G. Periaswami. Simultaneous measurement of emf and short circuit current for a potentiometric sensor using perturbation technique, Sensors and Actuactors B. 2005;104:94-102,

29. International Journal of Applied Power Engineering (IJAPE).2021;10(1):80-88. ISSN: 2252-8792, DOI: 10.11591/ijape.v10.i1.pp80-88

APPENDIX A : ARDUINO CODE

```
#include <LiquidCrystal.h>
#include "max6675.h"
#include <Wire.h>
#include <U8g2lib.h>
LiquidCrystal lcd(12,8,5,4,3,2);
int OxyPin = A0; //Oxygen pin is A0
int thermoDO = 7; //Digital pin D7
int thermoCS = 13; //CS pin is 13
int thermoCLK = 6; //Ok
float temperature = 0.0;//Define temperature
char disp;
MAX6675 thermocouple(thermoCLK, thermoCS, thermoDO);
int vccPin = 3;
int gndPin = 2;
float oxyPercent; //Oxygen
float eO2=0.0; //Analog voltage developped by the lambda sensor
float To2=600.0; //Working temperature of the lambda sensor
#define F 96485.34  //Define the Faraday constant
#define R 8.314  // Define the constant gases
#define O2Air 20.96  //Define Oxygen concentration in clean air
#define T0 273.2  // Define temperature in K
#define z 1.6*pow(10,-19) //Electronic charge
float Tom = 0.0;//Time of measure
void setup() {Serial.begin(9600);
// Max 6675 setup
pinMode(vccPin, OUTPUT); digitalWrite(vccPin, HIGH);
pinMode(gndPin, OUTPUT); digitalWrite(gndPin, LOW);
//End setup for Max 6675
//Setup LCD display
lcd.begin(20,4); //LCD's number of columns and rows:
lcd.clear();
lcd.print("Powering on. Please wait...");
delay(1500); //Give 1s to read
lcd.clear();
lcd.print("Lambda sensor calibration in progress");
delay(1500); //Give reader 1.5 second to read the display}
void loop()
{ temperature = thermocouple.readCelsius()+273.15; //Temperature is converted in K
//Oxygen with Lambda sensor
eO2 = analogRead(OxyPin);
To2=temperature;  oxyPercent  =  205*(O2Air*(exp((-(z*F*eO2)/(R*To2)))/1023.0*5.0));  //Temperature
is converted in K
// Calculate Oxygene concentration according to equation derived from the Nerst Law
//We now display T and 02
lcd.clear(); // Clear LCD to avoid weird characteres display
lcd.setCursor(0,0);
lcd.print("Temperature ");
lcd.print(temperature,1); //Display Reactor temperature with 1 decimal
lcd.print("K ");
//Display O2 in %
lcd.setCursor(0,1);
lcd.print("Oxygene ");
lcd.print(oxyPercent, 1); // Print Oxygen content on LCD
lcd.print("%");
//Display what is the time elapsed?
```

```
lcd.setCursor(0,2);
lcd.print("Time of measure ");
unsigned long currentMillis = millis();
Tom = ((currentMillis/1000)/60.0);
lcd.print(Tom,1);
lcd.print("mn");
// End calculating and displaying other parameters
delay(intervalHigh); }; // End loop
```

© 2024 Salou et al.; This is an Open Access article distributed under the terms of the Creative Commons Attribution License (http://creativecommons.org/licenses/by/4.0), which permits unrestricted use, distribution, and reproduction in any medium, provided the original work is properly cited.

Peer-review history:
The peer review history for this paper can be accessed here:
https://www.sdiarticle5.com/review-history/112025